Desalination and Water Treatment
www.deswater.com

doi: 10.5004/dwt.2019.23430

142 (2019) 260–271
February

Synthesis of polyacrylonitrile/graphene oxide nanocomposite for the removal of Cd(II) and Pb(II) from aqueous solutions

Adel A. El-Zahhar[a,b], K.S. Al-Namshah[c], Nasser S. Awwad[a,*]

[a]*Department of Chemistry, Faculty of Science, KKU, Abha 9004, Saudi Arabia, Tel. +966563764476; emails: aawwad@kku.edu.sa (N.S. Awwad), adelelzahhar@yahoo.com (A.A. El-Zahhar)*
[b]*Department of Nuclear Chemistry, EAEA, P.C. 13759, Cairo, Egypt*
[c]*Department of Chemistry, Faculty of Science for Girls, KKU, Abha 9004, Saudi Arabia; email: kalnmshah@kku.edu.sa*

Received 21 June 2018; Accepted 5 November 2018

ABSTRACT

Composite adsorbent polyacrylonitrile/graphene oxide (PAN/GO) was synthesized by grafting chemical polymerization of acrylonitrile in the presence of GO nanoplatelet. The GO was prepared from activated carbon prepared from date pits and distributed within the polymeric network as nanoplatelet which was reflected on the improved adsorption performance. The synthesized PAN/GO composite (GO content of 14%) was characterized using fourier transformed infrared, scanning electron microscopy-energy dispersive X-ray spectroscopy, and XRD. The adsorptive removal of Cd(II) and Pb(II) onto PAN/GO was studied at varied affecting conditions. The higher adsorption obtained are 72.04% and 81.27% for Cd(II) and Pb(II), respectively. Adsorption kinetic and isotherm models studies showed considerable fitting with pseudo-second-order and Langmuir models. The results obtained from the thermodynamic parameters confirmed the spontaneous nature of the process. The prepared PAN/GO composite adsorbent proved potential removal of Cd(II) and Pb(II) with adsorbed amount 14.07 and 11.17 mg/g, respectively.

Keywords: Polyacrylonitrile; Graphene oxide; Composite; Cadmium; Lead

1. Introduction

A critical environmental pollution hazard arises from the discharge of industrial wastewater flow out, containing high concentrations of heavy metals. Industrial wastewater containing heavy metals include metal-finishing, mining/metallurgical works. Cadmium and lead are classified as serious pollutants causing environmental problems. Cadmium danger and harming uncover a large number of indications as hypertension, renal issues, and blood infection. The contamination with Cd(II) is created from various modern methodologies such as the electroplating, batteries ventures, passing on, strands material, and synthetic compounds handling. As for lead, it is known to cause kidney disappointment, obliterating liver cells, interference of cell task and causes cerebrum disease. The impacts of lead harming incorporate iron deficiency, cerebral pain, and numerous unsafe maladies [1,2]. Lead fundamentally released into the earth from leaded fuel, lead mining enterprises, lead containing channels in water pipe frameworks, toxic painting materials, and coal.

Therefore, a potential removal studies must be performed for decontamination of waste streams from the hazardous metal ions and saving environment and human life. Different methods were studied for decreasing heavy metal ions concentrations in wastewater before discharging to the environment including chemical precipitation, ion exchange, membrane techniques, adsorption, etc. The connected system is subject to the type of waste, kind of contaminants, grouping of contaminants, process proficiency, and expenses. The overwhelming metals' purification was possibly examined utilizing distinctive minimal effort materials as: charcoal,

* Corresponding author.

coconut shell, and blend of carbon and limestone with significant effectiveness [3,4]. Agricultural wastes were considered as an exceptionally plentiful adsorbent materials for Cd(II) [5], with most extreme adsorption of 195.5 mg/g at pH 4 at 30°C. Distinctive adsorbent materials were conceivably examined as adsorbents for Cd(II) from squander arrangements [6–10] as: dirt minerals, zeolites, plants wastes, biomaterials, inorganic materials, muck, and carbonaceous materials.

Common bentonite was considered for cleaning of Cu(II) and Pb(II) [11] and demonstrated balance adsorbed measures of 57.8 and 21.1 mg/g for Pb(II) and Cu(II), individually. Additionally chitosan-bentonite composite was contemplated for adsorption of Pb(II) and Cu(II) from squander streams [12]. Regular minerals were connected for adsorption of perilous metals and demonstrated potential adsorption for Pb(II) and Cu(II) from solution [13–15]. Highly efficient removal of inorganic pollutants, such as toxic- and nuclear waste-related metal ions, remains the main task from the biological and environmental standpoint because of their harmful effects on the environment. Highly porous metal–organic frameworks, with excellent chemical stability and abundant functional groups, have represented a new addition to the area of the removal of various types of hazardous metal ion pollutants [16], such as boron nitride (BN) with a structure similar to graphene possesses many extraordinary properties such as high surface areas, high oxidization resistance with high chemical stability at high temperature. BN-based materials can be easily regenerated by burning in air. The BN-based materials have satisfactory sorption capacities for inorganic pollutants (e.g., heavy metal ions) and organic pollutants (e.g., dyes and pharmaceutical molecules) [17]. Polymer-based nanocomposites often present superior physical, chemical, and mechanical properties, as well as superior compatibility, as compared with single polymers, by incorporating the advantages of both counterparts in the composites [18].

Graphene oxide (GO) polymer composite was arranged and considered for expulsion of natural color [19]. The readied composite with 3% GO content demonstrated adsorption effectiveness of 99.7%.

GO is a carbonaceous material containing powerful practical gatherings as hydroxyl, epoxy, carbonyl, and carboxyl, which could be incorporated into adsorption process [20] by means of hydrogen holding, van der Waals powers, and hydrophilic collaborations. GO has discovered wide applications in various fields [21–25]. What's more nanostructure GO has more favorable circumstances as high adsorption proficiency, high soundness over wide pH range, and simplicity of scattering in arrangements. The adsorption of organic dyes from their solutions was studied and showed more efficient removal than graphene [26]. Polyacrylonitrile (PAN) was known with chemical, thermal, and granular stability, so found many applications for supporting fine adsorbent materials.

A new granular adsorbent material was prepared from GO (prepared from date pits activated carbon) and PAN. The prepared PAN/GO composite adsorbent was analyzed via XRD, scanning electron microscopy-energy dispersive X-ray spectroscopy, and fourier transformed infrared (FTIR). The synthesized composite was applied for adsorption of Cd(II) and Pb(II) from aqueous systems. The affecting conditions as ion concentration, pH, contact time, and adsorbent dose were assayed. Kinetic and isotherm models were considered with resultant information for proposing the procedure component.

2. Experimental

2.1. Materials

The graphene powder used in the preparation was obtained from date pits activated carbon by modified Hammer's procedure [27]. 5 g of date pits activated carbon with 2.5 g $NaNO_3$ and 115 ml H_2SO_4 were mixed in ice shower for 30 min took after by mixing at room temperature. Potassium permanganate (15 g) was included moderate, trailed by sonication at 40°C for 2 h. In the wake of acquiring a pale issue, 500 ml of distilled water was included gradually with blending for 60 min. Hydrogen peroxide 10 ml (30%) included and blending was proceeded for 2 h. At last, the response blend was sonicationed, centrifuged, and washed a few times for evacuating pollutions. GO was dried at 85°C for 24 h and described. Acrylonitrile and ammonium persulfate were provided by Sigma-Aldrich. The synthetic concoctions were utilized as gotten.

2.2. Procedures

2.2.1. Synthesis of GO-PAN composite adsorbent

Appropriate amount of GO (to obtain 14 wt%) was suspended in acrylonitrile solution (35 wt%) in dimethylformamide. The mixture was kept under stirring for 30 min with nitrogen deaeration, then the initiator ammonium persulfate was added. The obtained composite was washed by acetone to remove unreacted monomer and dried at 70°C.

2.3. Characterizations

The prepared GO-PAN composite was analyzed using FTIR spectroscopy using NICOLET 6700 FTIR Thermo Scientific, and its surface morphology was analyzed using Jeol Model 6360 LVSEM, USA, scanning electron microscope (SEM). The crystal structure of the composite was studied using Schimadzu 6000DX XRD unit.

2.4. Adsorption experiments

The removal of Pb(II) and Cd(II) individually onto GO-PAN composite were studied as follows: appropriate weight of GO-PAN was mixed with 20 ml metal ion solution of 50 mg/L for certain time periods. The concentration of either Pb(II) or Cd(II) before and after experiments was measured using induction-coupled plasma optical emission spectroscopy (Thermo Scientific, Part No: 1340910, Qtegra Soft ware, Germany). The affecting experimental conditions were studied, where the amount adsorbed of either Pb(II) or Cd(II) (mg/g) onto GO-PAN was calculated as:

$$q_e = \left(C_o - C_e\right) \times \frac{V}{m} \tag{1}$$

where q_e is the adsorbed (mg/g); C_o and C_e are the initial and final ion concentrations (mg/L), respectively; m is the adsorbent amount (g); and V is the volume of solution (L).

The effect aqueous solution pH on the adsorption of Pb(II) and Cd(II) GO-PAN was studied, where varied solutions pH were adjusted by adding drops of 0.01 M HCl or 0.01 M NaOH. The ionic strengths were adjusted with 0.01–1 M NaCl solution at certain values.

3. Results and discussion

3.1. Characteristics of GO-PAN

The FTIR analysis of GO-PAN showed a absorption at 3,420 cm^{-1} allocated for water molecules OH groups, while the peaks 2,900, 1,600, 1,500, and 800 cm^{-1} are assigned to C=C, C=N, N–O, and amine, respectively, in the polymer moiety. The presence of these peaks reflects that the GO was successfully combined within the polymer matrix.

The SEM images for the prepared GO-PAN and GO-PAN-Cd(II) are given in Fig. 1. The micrograph of GO-PAN shows a rough and microporous structure surface of GO-PAN, while the micrograph of GO-PAN-Cd(II) clearly shows a different surface as a result of Cd(II) presence. The SEM micrograph confirms the exfoliation of polymer within the layers with regular structures and a porous surface morphology appeared before metal ion adsorption. The SEM micrograph for GO-PAN-Cd(II) shows a relatively smooth surface with different porosity and surface morphology. The energy dispersive X-ray spectroscopy chart for either GO-PAN or GO-PAN-Cd(II) shows the elemental content in the composite and Cd(II) in the composite after adsorption as shown in Fig. 2.

The XRD patterns for GO-PAN and GO-PAN-Cd(II) are given in Fig. 3. The figure shows the characteristic peak of GO but with low intensity due to the presence of low GO

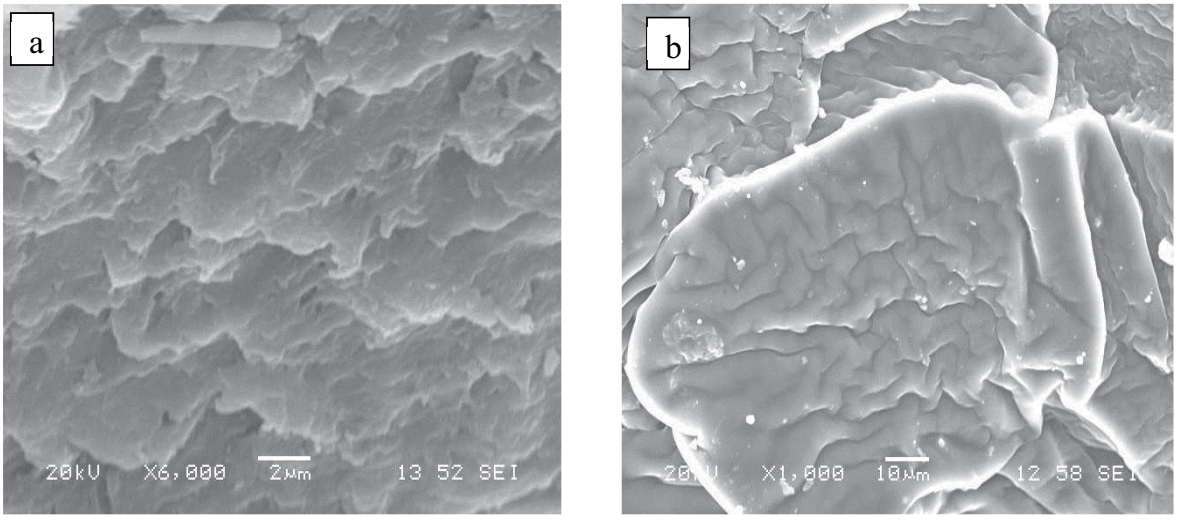

Fig. 1. SEM images of GO-PAN (a) and GO-PAN-Cd(II) (b).

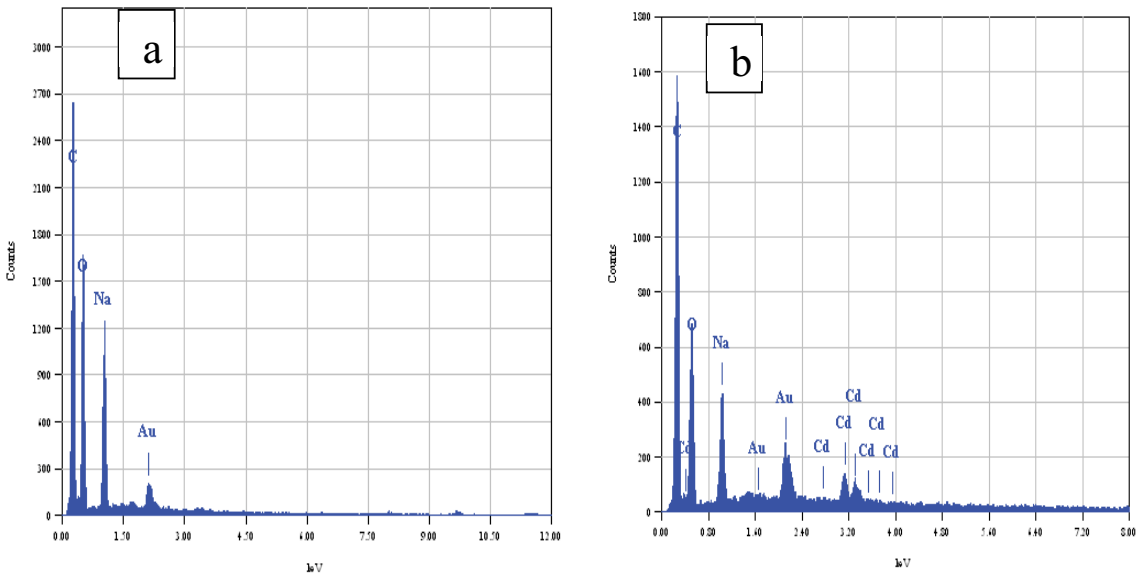

Fig. 2. EDX charts for GO-PAN (a) and GO-PAN-Cd(II) (b).

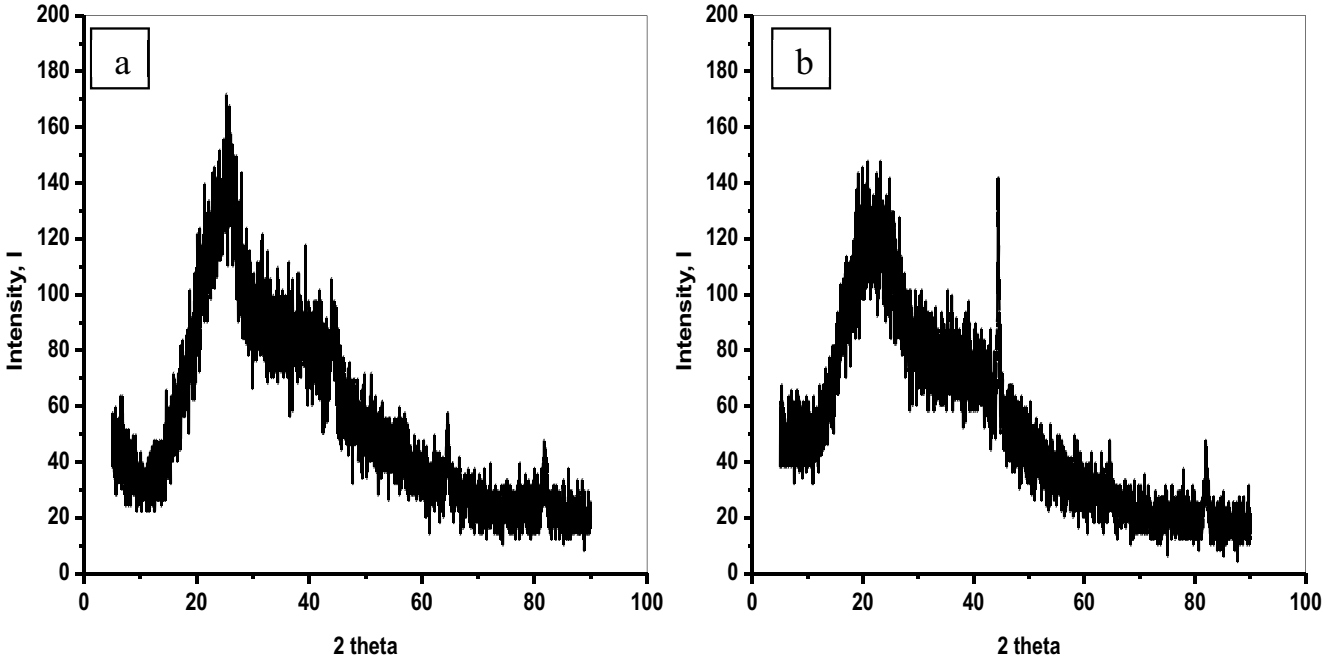

Fig. 3. XRD patterns for GO-PAN (a) and GO-PAN-Cd(II) (b).

content in the composite. The slight shift in peaks positions reflects that the polymer was formed in the interlayer distance [28,29]. The results in XRD patterns of GO-PAN-Cd(II) show the appearance a new peak as a result of Cd(II) presence and confirming the intercalation/exfoliation of the polymer within the oxide. This finding would expect to enhance the adsorption behavior of the composite adsorbent.

3.2. Adsorption characteristics

3.2.1. Effect of mixing time

The contact period between aqueous solution containing either Cd(II) or Pb(II) and GO-PAN was varied. The results given in Fig. 4 proved 60 min of contact is adequate for the reaction, as the removal percentage show no marked increase with increasing contact time. So, the appropriate a contact period is 60 min for further experiments.

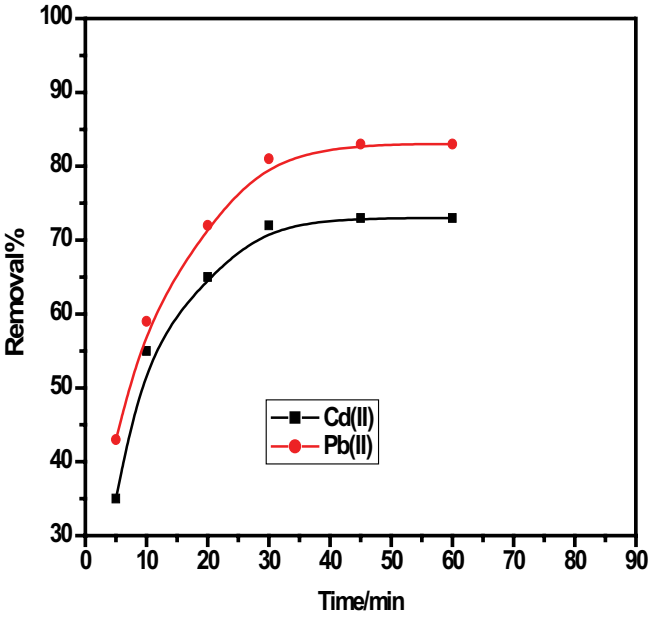

Fig. 4. Effect of contact time on the adsorption of Cd(II) and Pb(II) on GO-PAN, Cd(II), and Pb(II) is 50 mg/L and composite dose is 10 g/L and pH is 4.7.

3.2.2. Effect of pH and ionic strength

The aqueous solution pH has a considerable effect on the speciation of metal ions. It is clear that the uptake of both Pb(II) and Cd(II) individually onto GO-PAN increased with increasing the solution pH within the studied pH range. The results presented in Fig. 5 that show that the uptake of Pd(II) increases suddenly as the pH increases from 2 to 6, while slowly increase with pH up to 7. The uptake of Cd(II) shows nearly the same behavior but with a lower uptake. In both cases, the maximum adsorption was observed at pH between 6 and 7.

It is reported that the surface charge of PAN-GO within the studied pH range is negative [30]. PAN-GO negative surface charge increase with increasing pH, which highly increase the adsorption of Pb(II) and Cd(II). This finding could be explained by increasing the electrostatic attraction between PAN-GO surface groups and metal ions [31]. It was found that at higher pH, the adsorption efficiency of M^+ positively enhanced. In addition, the predominant species of metal ions in aqueous solution at higher pH are hydrolyzed. The effect of pH announce that the surface complexation mechanism takes part in the adsorption process [32]. The adsorption efficiency of Pb(II) and Cd(II) onto PAN-GO is comparable

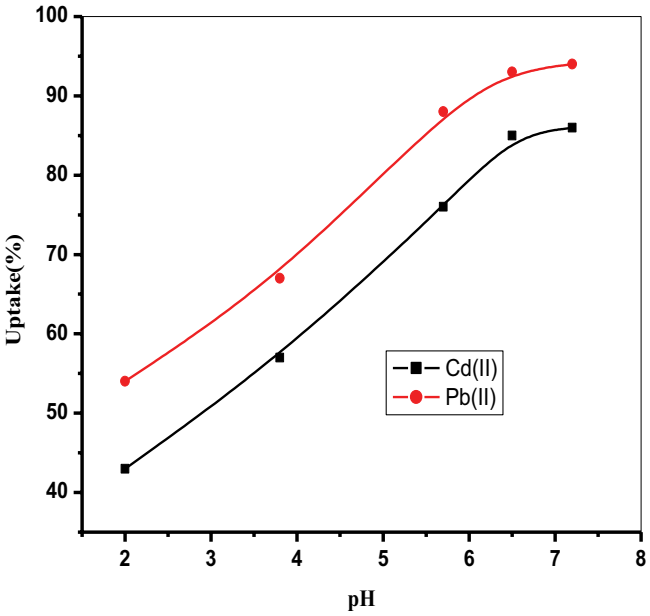

Fig. 5. Effect of solution pH on the adsorption of Cd(II) and Pb(II) on GO-PAN, Cd(II), and Pb(II) is 50 mg/L and composite dose is 10 g/L.

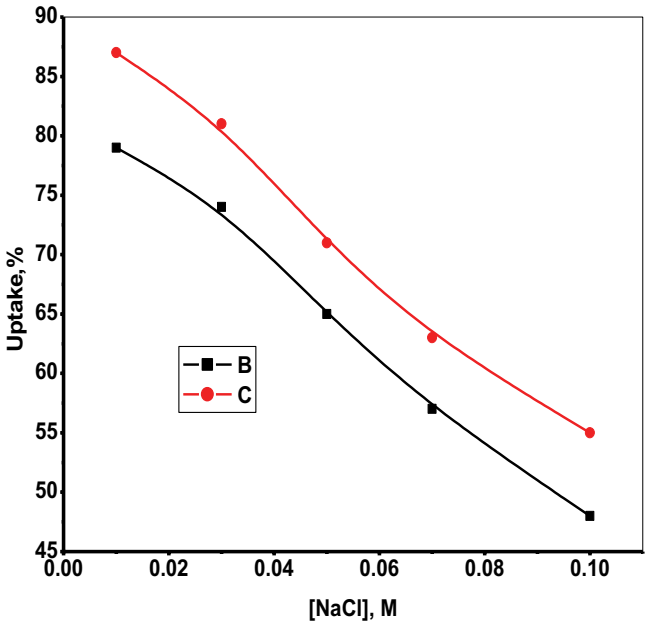

Fig. 6. Effect of ionic strength on the adsorption of Cd(II) and Pb(II) on GO-PAN, Cd(II), and Pb(II) is 50 mg/L and composite dose is 10 g/L.

with previous studies as the content of GO is 14% within the composite. The active component in the composite is 14% GO. The role of PAN is a supporting agent for granulation of the produced composite and enhancing the mechanical and physical properties. So, it is worth mention that PAN-GO with 14% GO shows a comparable adsorption efficiency compared with GO alone [33,34].

The effect of ionic strength on the adsorption of Pb(II) and Cd(II) onto PAN-GO is determined by different concentrations of NaCl added to the aqueous solution from 0.01 to 0.1 M. The results presented in Fig. 6 show a distinct negative effect of ionic strength upon the uptake of metal ions. This observation could be explained on the bases of competitive effect of Na^+ with the studied ions, where at lower ionic strength a high surface function groups are available for targeted metal ions adsorption. This finding refers to the participation of cation exchange mechanism (chemical adsorption) part in the adsorption process [35].

3.2.3. Kinetics of adsorption

The amount of ions adsorbed onto the polymeric resin studied with time for estimating the adsorption mechanism. The results in Fig. 4 representing the removal percentage with time show that mixing period of 60 min is optimum for attaining the equilibrium and there is no more increase in removal percentage with time.

Different kinetic models were applied on the obtained results and the kinetic parameters were determined. The kinetic models correlate the amount adsorbed of ions with time. Lagergren presented the following equation for pseudo-first-order reactions [36]:

$$\frac{dq_t}{dt} = k_1\left(q_e - q_t\right) \tag{2}$$

as q_e and q_t are the ion concentration in solid phase at equilibrium and at time t, respectively, and k_1 is the model constant (min^{-1}). The linear form of the above equation was obtained by integration at the borders (q_t = 0 to $q_t = q_t$ and t = 0 to $t = t$) as:

$$log\left(q_e - q_t\right) = logq_e - \frac{k_1 t}{2.303} \tag{3}$$

The rate constant, k_1, was determined from the plot of $\log(q_e - q_t)$ with t (Fig. 7), while the value of q_e was determined Ffrom the intercept. The model variables with the coefficient are given in Table 1.

The plots in Fig. 7 show linear fit with correlation coefficient (R^2) of 0.976 and 0.990 for Cd-GO-PAN and Pb-GO-PAN adsorption systems, respectively. The values of k_1 for Cd-GO-PAN and Pb-GO-PAN are 0.0667 and 0.0555 min^{-1}, respectively. The calculated q_e for Cd-GO-PAN and Pb-GO-PAN systems were calculated to be 16.980 and 11.776 mg/g, correspondingly. The values of calculated adsorption capacity q_e and the linear regression coefficient clarify that the studied kinetic model could fit with the experimental results for Cd-GO-PAN, adsorption system, while this model can't fit the experimental results of Pb-GO-PAN system.

Second-order kinetic model that describe the chemical adsorption is given by [37]:

$$\frac{dq_t}{dt} = k_2\left(q_e - q_t\right)^2 \tag{4}$$

as k_2 is the model constant (g/mg min). The above equation could be integrated at the border (q_t = 0 to $q_t = q_t$ at t = 0 to $t = t$) to be:

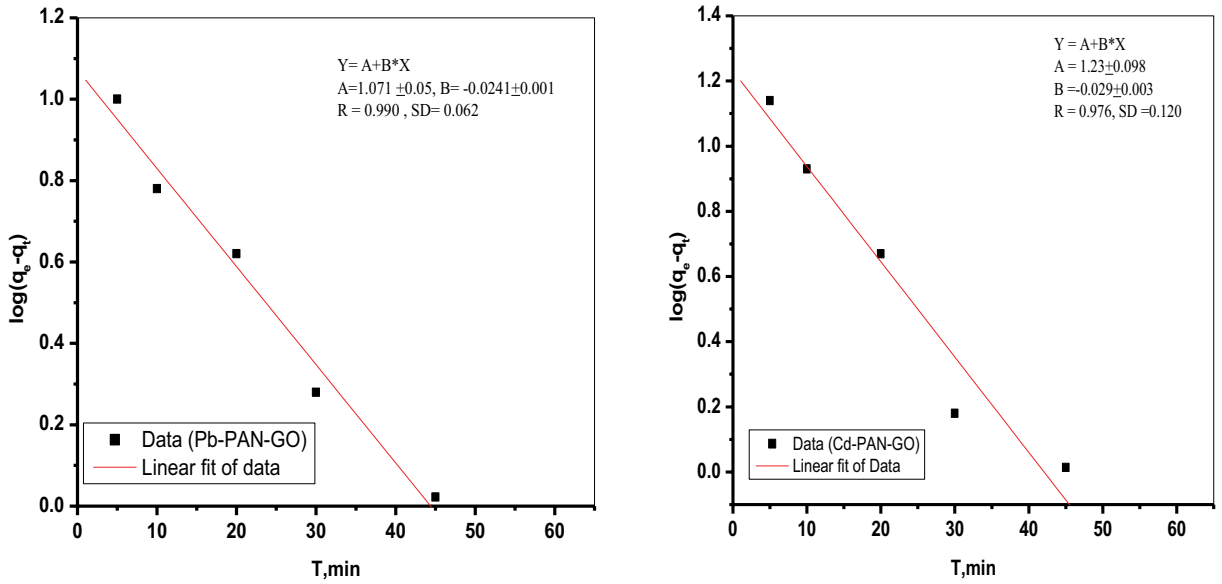

Fig. 7. Lagergren pseudo-first-order plot for the adsorption of Cd(II) and Pb(II) on GO-PAN.

Table 1
Kinetic models variables for the adsorption of Cd(II) and Pb(II) onto GO-PAN

Adsorption system	Kinetic model	Parameters	R^2	SD
Cd-GO-PAN	Pseudo-first-order	k_1 = 0.0667 q_e = 16.98	0.976	0.120
	Pseudo-second-order	k_1 = 1.35 × 10^{-3} q_e = 28.98	0.978	0.133
	Elovich	β = 0.0754 α = 18.116	0.985	1.039
	Intra-particle	k_{id} = 2.668 C = 3.09	0.991	0.834
Pb-GO-PAN	Pseudo-first-order	k_1 = 0.0555 q_e = 11.776	0.990	0.062
	Pseudo-second-order	k_1 = 6.34 × 10^{-3} q_e = 22.98	0.999	0.036
	Elovich	β = 0.1104 α = 15.727	0.991	0.550
	Intra-particle	k_{id} = 2.372 C = 6.166	0.982	0.776

$$\frac{t}{q_t} = \frac{1}{k_2 q_e^2} + \frac{t}{q_e} \tag{5}$$

The model variables were calculated from the plot of t/q_t with t (Fig. 8). The plot shows a linear relation, and the model parameters with the correlation coefficient R^2 were given in Table 1.

The results of the studied kinetic model clarify that the experimental results for the adsorption of Pb(II) onto GO-PAN could be described by kinetic model supporting chemical adsorption, but with respect to Cd(II)-GO-PAN could not. The sorption of Pb(II) could be favorably described by the pseudo-second-order kinetic model. This finding clarifies that chemical adsorption is the predominant mechanism for Pb(II)-GO-PAN [38].

Elovich kinetic model was applied upon the results to explain mainly the chemisorptions onto heterogeneous solid surfaces. The linearized form of Elovich model equation is [39]:

$$q_t = \left(\frac{1}{\beta}\right)\ln(\alpha\beta) + \left(\frac{1}{\beta}\right)\log t \tag{6}$$

where α and β are model parameters representing the starting sorption rate (g mg^{-1} min^{-2}) and the leaching constant

(mg g^{-1} min^{-1}), correspondingly. The model parameters were calculated from the linear fit of q_t vs. log (t) plot in Fig. 9 and presented in Table 1.

The values of Elovich constant α = 18.11 g mg^{-1} min^{-2} and β = 0.0754 for Cd-GO-PAN, refereeing to the effect of adsorbent dose and the possibility of performing sorption–desorption regeneration cycles of adsorbent. The value of correlation coefficient (R^2 = 0.985) do not reflect a good fit of Elovich model with the experimental results of Cd-GO-PAN.

With respect to Pb-GO-PAN adsorption system, the values of Elovich model parameters α = 0.114 g mg^{-1} min^{-2} and β = 15.72 also reflect the same concept as Cd-GO-PAN system, while the correlation coefficient (R^2 = 0.990) for Pb-GO-PAN system reflects a higher possibility of fitting the experimental results with Elovich model than with Cd-GO-PAN.

It could be inferred that both chemical and surface adsorption mechanisms are participating in both Cd(II)-GO-PAN and Pb(II)-GO-PAN systems.

Intra-particle diffusion model was studied to explain the influence of the transfer of metal ions from solution to solid surface of adsorbent on the reaction. The adsorption reaction could be affected by film diffusion, pore diffusion, surface diffusion, and/or adsorption on pore surface. The studied batch experiment was performed with shaking, therefore, the transfer of adsorbate particles could be described by diffusion coefficient that gives a considerable fitting with the experimental results.

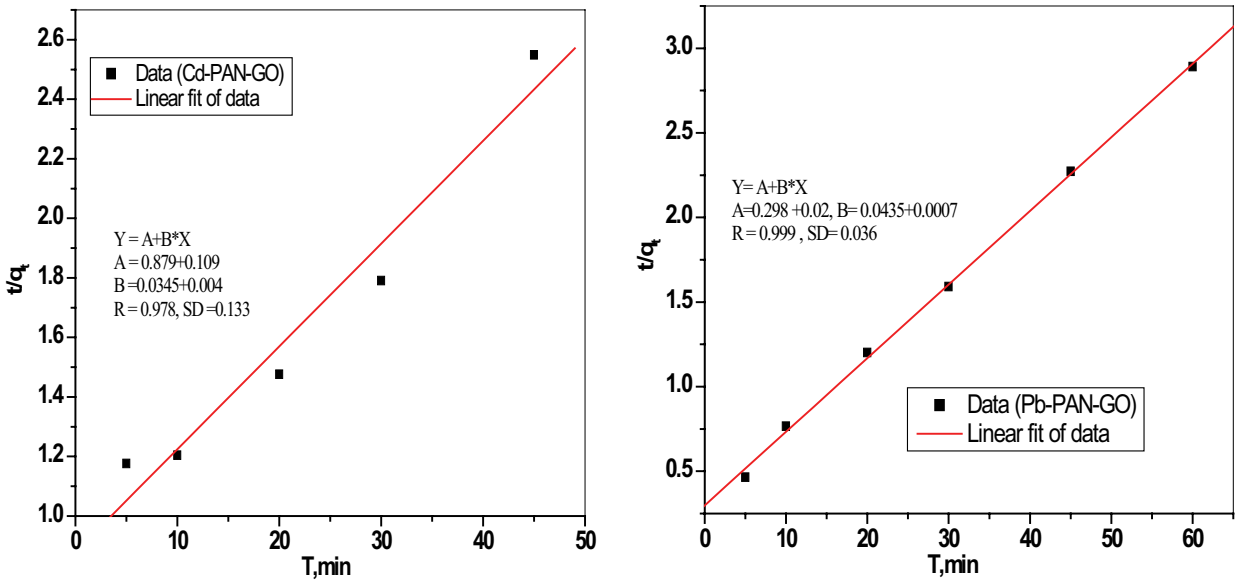

Fig. 8. Pseudo-second-order plot for the adsorption of Cd(II) and Pb(II) on GO-PAN.

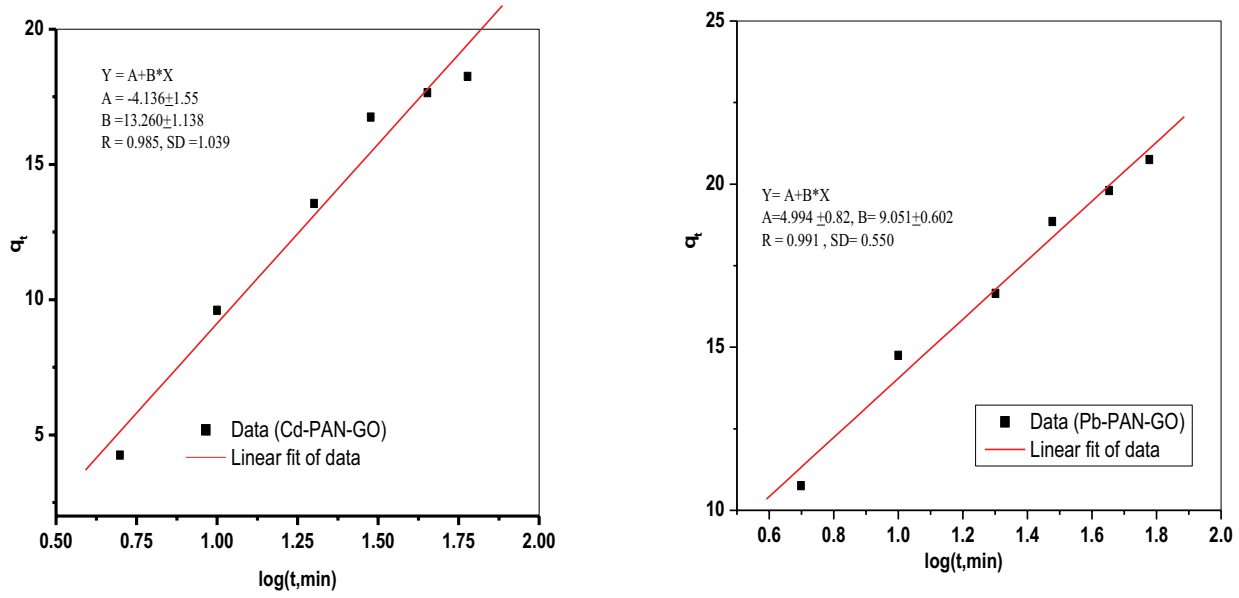

Fig. 9. Elovich model plot for the adsorption of Cd(II) and Pb(II) on GO-PAN.

Weber model could be studied to explain the intra-particle diffusion influence on the reaction by the following equation:

$$q_t = k_{id} t^{0.5} + C \quad (7)$$

where k_{id} is the Webber model constant (mg g^{-1} min$^{-0.5}$) and C is a constant (mg g^{-1}) connected to the depth of the boundary layer, which is reflecting the boundary layer effect.

If the adsorption takes place within multilayer adsorbent, the adsorbate particles have to spread within the interior pores of solid materials. The model parameters were obtained from the plot of q_t vs. $t^{1/2}$ in Fig. 10 and presented in Table 1.

The results in Fig. 10 show two linear regions referring to the participation of at least two steps in the reaction. The linearity in the first region refers to a diffusion of metal ions into macro-pores of adsorbent, while the second linear region showing that the adsorbate particles diffuse within a micro-pore of adsorbent.

The results in the figures reflect a variation of particle migration rate between different stages of sorption. The deviation of straight lines from the origin (when extrapolated) reflects that the diffusion within pore is not only the rate affecting step. The model variables for both Cd-GO-PAN and Pb-GO-PAN systems are given in Table 1. These results indicate that Webber diffusion model couldn't be considered as the controlling mechanism in the adsorption reaction.

3.2.4. Adsorption isotherm

The adsorption of Cd(II) and Pb(II) onto GO-PAN was studied at different initial ion concentrations (within the range 5–70 mg/L) for Cd(II) and Pb(II) individually. The removal and the adsorbed amount of both Cd(II) and Pb(II) were presented against the starting metal ion concentration in Fig. 11. The results show that the amount of either Cd(II) or

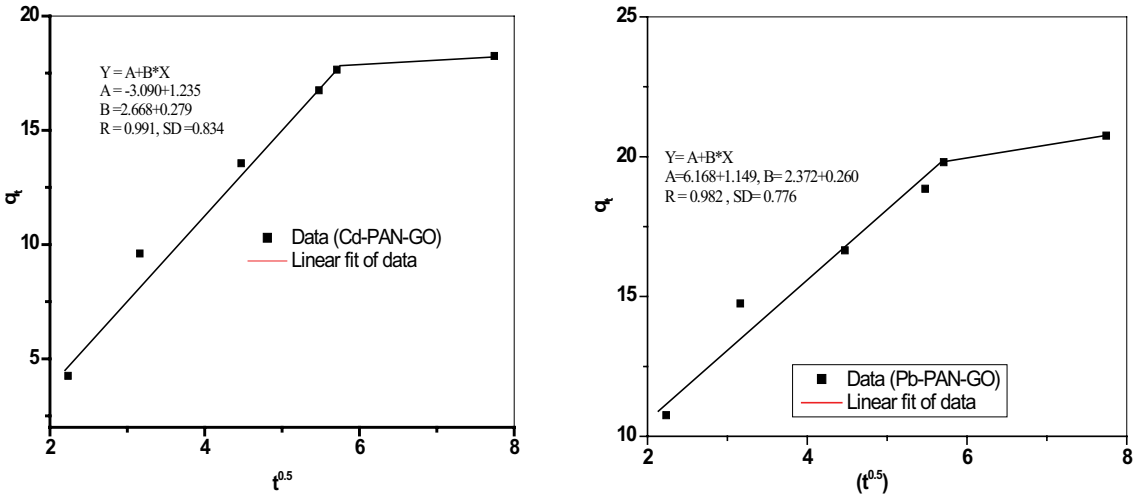

Fig. 10. Intra-particle diffusion model plot for the adsorption of Cd(II) and Pb(II) on GO-PAN.

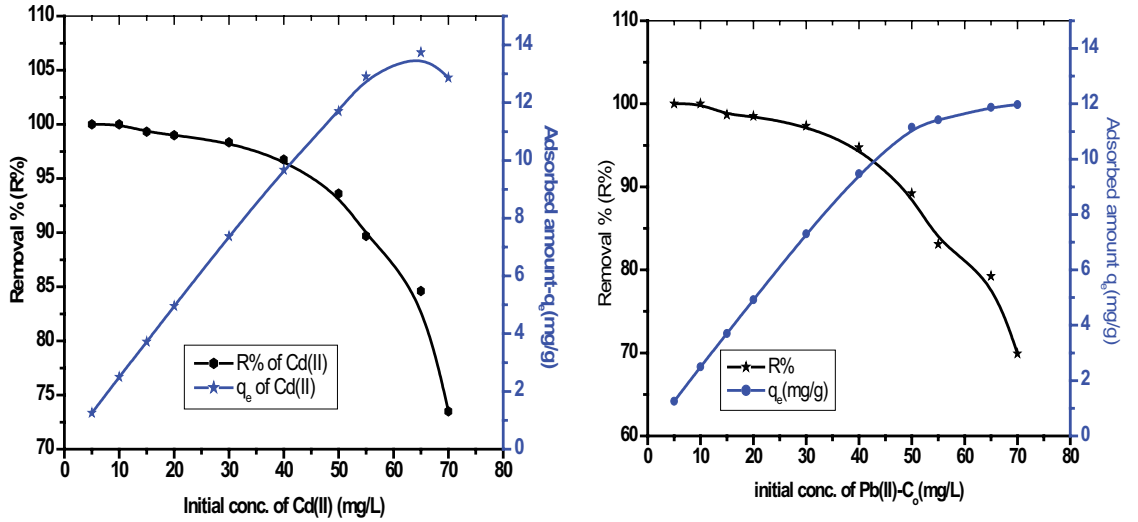

Fig. 11. Effect of ion concentration on the adsorption of Cd(II) and Pb(II) on GO-PAN and composite dose is 10 g/L, contact time 60 min, and pH is 4.7.

Pb(II) retained on the solid adsorbent increases with increasing ion concentration till 50 mg/L, then slightly decreases.

Different isotherm models were studied for describing the adsorption mechanism controlling the reaction. Langmuir isotherm model was studied for adsorption of Cd(II) and Pb(II) on GO-PAN, which expressed as:

$$\frac{C_e}{q_e} = \frac{1}{K_L} + \frac{C_e}{q_{\max}} \tag{8}$$

as C_e is the metal ion concentration in solution after experiment (mg/L), q_e is metal ion concentration on the solid adsorbent (mg/g), and $q_{\max}$ and K_L are model parameters connected to maximum adsorbed amount (mg/g) and adsorption energy, correspondingly. A plot of C_e is presented vs. C_e/q_e in Fig. 10 was constructed and the model variables were determined from the plot and given with coefficient R^2 in Table 2.

The values of R^2 for Cd(II)-GO-PAN and Pb(II)- GO-PAN systems were calculated to be 0.999 and 0.9999, respectively, reflecting that the adsorption results fit well with Langmuir isotherm as shown in Fig. 12. This finding supports monolayer chemical adsorption onto homogeneous surface with no adsorbate interaction.

Freundlich isotherm model was applied on the experimental results, which described by the following equation:

$$\log q_e = \log k_f + \frac{1}{n}\log C_e \tag{9}$$

as k_f (mg/g) and n are model constants, indicating the adsorption capacity and favorability nature of the adsorption process. Freundlich model constants were determined from the linear fit of log q_e vs. log C_e plot in Fig. 13 and given with the correlation coefficient in Table 2.

The values of R^2 of Freundlich plots for Cd(II)-GO-PAN and Pb(II)- GO-PAN systems were calculated to be 0.971 and 0.962, respectively, explaining a bad fit of the experimental results with Freundlich isotherm model.

Table 2
Adsorption isotherm models parameters for Cd(II)-GO-PAN and Pb(II)-GO-PAN systems

Model	Parameter	Cd(II)-GO-PAN	Pb(II)-GO-PAN
Langmuir	$q_{\max}$	13.31	12.25
	K_L	44.05	23.20
	R_2	0.999	0.999
	SD	0.0233	0.0074
Freundlich	$1/n$	0.284	0.264
	K_f	8.016	6.71
	R_2	0.971	0.962
	SD	0.045	0.059
Dubinin–Radushkevich	B	–0.463	–0.508
	$q_{\max}$	11.78	10.95
	E_s	1.01	1
	R_2	0.958	0.978
	SD	0.151	0.112

Dubinin–Radushkevich (D-R) adsorption isotherm model was studied, which describes the adsorption onto porous solid surfaces, and described the following equation [40]:

$$\ln q_e = \ln q_{\max} - \beta\varepsilon^2 \tag{10}$$

where β is D-R model constant (mol²/kJ²), $q_{\max}$ is constant referring to the maximum adsorbed amount (mg/g), and ε is Polanyi potential (ε = RTln(1 + 1/C_e). The D-R model constants were obtained from the linear fit of the plot of lnq_e vs. ε² (Fig. 14) and are given with correlation coefficient in Table 2. The adsorption free energy (E_S) is calculated as:

$$E_S = \left(-2\beta\right)^{-1/2} \tag{11}$$

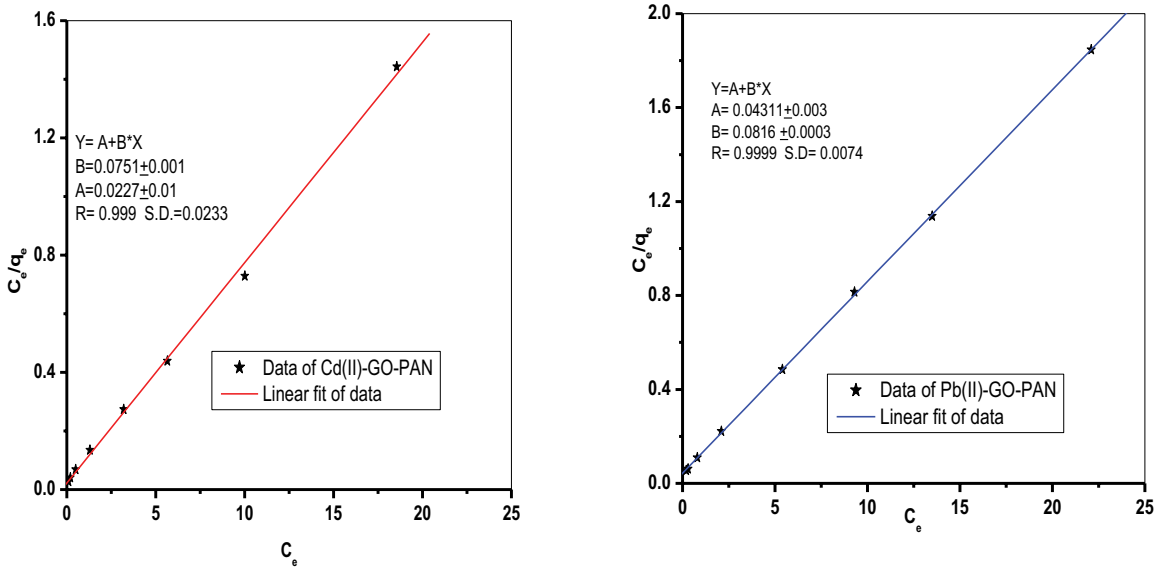

Fig. 12. Langmuir isotherm model plot for the adsorption of Cd(II) and Pb(II) on GO-PAN.

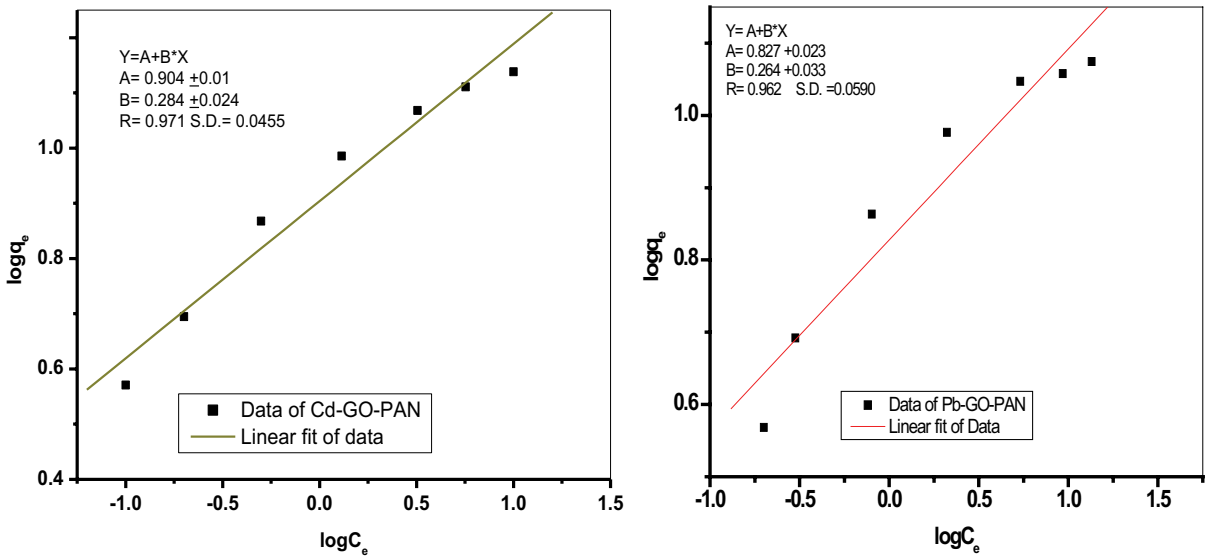

Fig. 13. Freundlich isotherm model plot for the adsorption of Cd(II) and Pb(II) on GO-PAN.

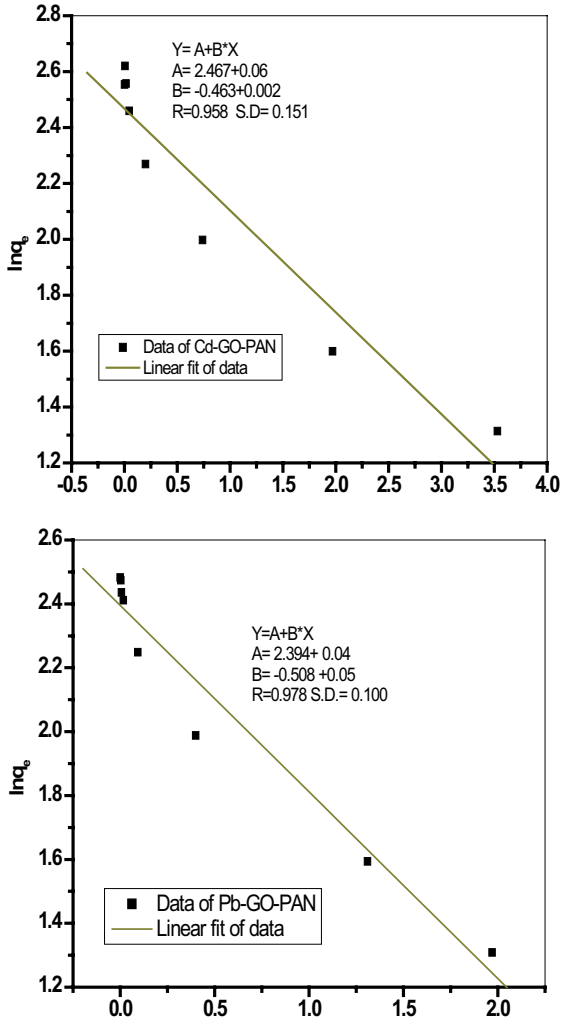

Fig. 14. D-R isotherm model plot for the adsorption of Cd(II) and Pb(II) on GO-PAN.

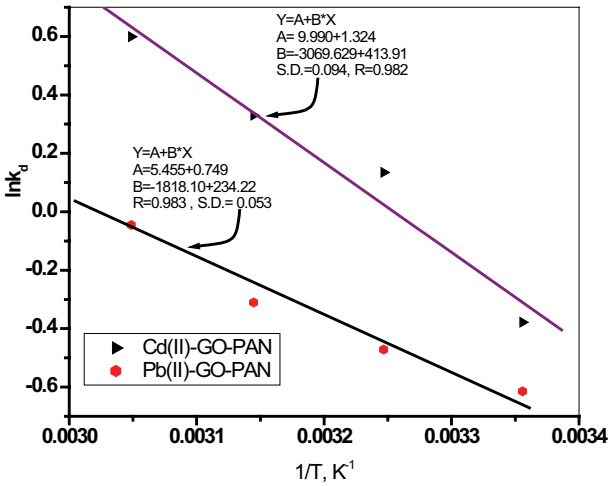

Fig. 15. Van't Hoff plot for the adsorption of Cd(II) and Pb(II) on GO-PAN.

The calculated mean adsorption free energy (E_S) from D-R model for the adsorption of Cd(II) and Pb(II) is 1.04 and 1 kJ/mol, respectively. These values reflect that physical adsorption is a participating mechanism [41].

3.2.5. Thermodynamic studies

The reaction of Cd(II) and Pb(II) with GO-PAN was tested at varied temperatures within 25°C–60°C. The portioning of metal ion between solution and solid phase was represented against the reciprocal of absolute temperature (Fig. 15). The thermal variables change in Gibbs free energy (ΔG°), enthalpy (ΔH°), and entropy (ΔS°) were determined by the following equations:

$$\log k_d = \frac{\Delta S^\circ}{2.303R} - \frac{\Delta H^\circ}{2.303RT} \quad (12)$$

Table 3
Thermal variables for the adsorption of Cd(II) and Pb(II) onto GO-PAN

Temperature (°K)	Thermodynamic parameters for Cd-GO-PAN			Thermodynamic parameters for Pb-GO-PAN		
	ΔG^o (kJ/mol)	ΔS^o (J/mol.K)	ΔH^o (kJ/mol)	ΔG^o (kJ/mol)	ΔS^o (J/mol.K)	ΔH^o (kJ/mol)
298	0.936	191.27	58.77	1.522	104.44	34.81
308	–0.344			1.207		
318	–0.872			0.819		
328	–1.663			0.122		

$$\Delta G^\circ = -RT \ln k_d \quad (13)$$

where k_d is the portioning coefficient, determined as:

$$k_d = \frac{q_e}{C_e} \quad (14)$$

and R is gas constant (8.314 J/mol/K) and T is the temperature (°K). The values of thermal variables were determined and are given in Table 3.

The sign of ΔH° indicates the endothermic behavior of the reaction of either Cd(II) or Pb(II) on GO-PAN, while the positive ΔS° refer to higher degree of freedom on solid surface with the reaction. The small absolute value of ΔG^o shows the feasibility and spontaneity of the reaction and, furthermore, the negative values of DG_{ads} also show the strong interaction of the inhibitor molecule onto the Cd(II) or Pb(II) surfaces and indicate the participation of physical adsorption mechanism in the process [42].

4. Conclusion

GO-PAN-GO-PAN composite adsorbent was prepared, analyzed, and studied for the adsorption of Cd(II) and Pb(II). The equilibrium adsorption results showed that GO-PAN composite of 14% GO with dosage 10 g/ml, 25°C, and a time of 24 h give adsorption capacity of 14.07 and 11.17 mg/g for Cd(II) and Pb(II), correspondingly. The adsorption reaction could follow the pseudo-second-order kinetics, reflecting the major participation of chemical adsorption mechanism. The isothermal studies showed that the removal of Cd(II) and Pb(II) on GO-PAN fit well with Langmuir model, supporting monolayer chemical adsorption onto homogeneous surface. The calculated thermal variables suggest that the adsorption of Cd(II) and Pb(II) on GO-PAN is endothermic and feasible. Based on the above, GO-PAN could be potentially applied for adsorption of hazardous metal ions from aqueous systems. Also, it was found that both physical and chemical adsorptions contribute at the mechanism of sorption.

Acknowledgment

The authors extend their appreciation to the Deanship of Scientific Research at King Khalid University for funding this work through research groups program under grant number R.G.P.1/23/38.

References

[1] R. Naseem, S.S. Tahir, Removal of Pb(II) from aqueous solution by using bentonite as an adsorbent, Water Res., 35 (2001) 3982–3986.
[2] B. Das, N.K. Mondal, Calcareous soil as a new adsorbent to remove lead from aqueous solution, equilibrium kinetic and thermodynamic study, Univ. J. Environ. Res. Technol., 1 (2011) 515–530.
[3] H.A. Aziz, M.N. Adlan, C.S. Hui, M.S.M. Zahari, B.H. Hameed, Removal of Ni, Cd, Pb, Zn and colour from aqueous solution using potential low cost adsorbent, *Indian J. Eng. Mater. Sci*., 12 (2005) 248–258.
[4] O. Yavuz, R. Guzel, F. Aydin, I. Tegin, R. Ziyadanogullari, Removal of cadmium and lead from aqueous solution by calcite, *Pol. J. Environ. Stud*., 16 (2006) 467–471.
[5] Z. Al Othman, A. Hashem, M.A. Habila, Kinetic, equilibrium and thermodynamic studies of cadmium (II) adsorption by modified agricultural wastes, Molecules, 16 (2011) 10443–10456.
[6] L. Semerjian, Equilibrium and kinetics of cadmium adsorption from aqueous solutions using untreated Pinus halepensis sawdust, J. Hazard. Mater., 173 (2010) 236–242.
[7] Z.Z. Li, T. Katsumi, S. Imaizumi, X.W. Tang, T. Inui, Cd(II) adsorption on various adsorbents obtained from charred biomaterials, J. Hazard. Mater., 183 (2010) 410–420.
[8] F.Y. Wang, H. Wang, J.W. Ma, Adsorption of cadmium (II) ions from aqueous solution by a new low-cost adsorbent-bamboo charcoal, J. Hazard. Mater., 177 (2010) 300–306.
[10] H.R. Tashauoei, H.M. Attar, M.M. Amin, M. Kamali, M. Nikaeen, M.V. Dastjerdi, Removal of cadmium and humic acid from aqueous solutions using surface modified nanozeolite A, Int. J. Environ. Sci. Technol., 7 (2010) 497–508.
[10] M. Visa, C. Bogatu, A. Duta, Simultaneous adsorption of dyes and heavy metals from multicomponent solutions using fly ash, Appl. Surf. Sci., 256 (2010) 5486–5491.
[11] B. Sadeghalvad, M. Torabzadehkashi, A.R. Azadmehr, A comparative study of Cu(II) and Pb(II) adsorption by Iranian bentonite (Birjand area) in aqueous solutions, Adv. Environ. Technol., 2 (2015) 93–100.
[12] C.M. Futalan, C.C. Kan, M.L. Dalida, K.J. Hsien, C. Pascua, M.W. Wan, Comparative and competitive adsorption of copper, lead, and nickel using chitosan immobilized on bentonite, Carbohydr. Polym., 83 (2011) 528–536.
[13] B. Sadeghalvad, H.S. Karimi, H. Hosseinzadegan, A.R. Azadmehr, A comparative study on the removal of lead from industrial wastewater by adsorption onto raw and modified Iranian bentonite (from Isfahan area), Desalin. Water Treat., 52 (2014) 6440–6452.
[14] B. Sadeghalvad, M. Armaghan, A. Azadmehr, Using Iranian bentonite (Birjand area) to remove cadmium from aqueous solutions, Mine Water Environ., 33 (2014) 79–88.
[15] Y. Liu, X. Shen, Q. Xian, H. Chen, H. Zou, S. Gao, Adsorption of copper and lead in aqueous solution onto bentonite modified by 4′-methylbenzo-15-crown-5, J. Hazard. Mater., 137 (2006) 1149–1155.
[16] J. Li, X. Wang, G. Zhao, C. Chen, Z. Chai, A. Alsaedi, T. Hayat, X. Wang, Metal–organic framework-based materials: superior adsorbents for the capture of toxic and radioactive metal ions, Chem. Soc. Rev., 47 (2018) 2322–2356.

[17] S. Yu, X. Wang, H. Pang, R. Zhang, W. Song, D. Fu, T. Hayat, X. Wang, Boron nitride-based materials for the removal of pollutants from aqueous solutions: a review, Chem. Eng. J., 333 (2018) 343–360.
[18] G. Zhao, X. Huang, Z. Tang, Q. Huang, F. Niu, X. Wang, Polymer-based nanocomposites for heavy metal ions removal from aqueous solution: a review, Polym. Chem., 9 (2018) 3562–3582.
[19] J. Qin, F. Qiu, X. Rong, H. Zhao, D. Yang, J. Wan, Preparation of graphene oxide/polyurethane foam material and its removal application of malachite green from aqueous solution, J. Appl. Polym. Sci., 131 (2014) 1–9, doi: 10.1002/APP.40988.
[20] D.R. Dreyer, S. Park, C.W. Bielawski, R.S. Ruoff, The chemistry of graphene oxide, Chem. Soc. Rev., 39 (2010) 228–240.
[21] X.J. Yang, Y. Makita, Z.H. Liu, K. Ooi, Novel synthesis of layered graphite oxide birnessite manganese oxide nanocomposite, Chem. Mater., 15 (2003) 1228–1231.
[22] G.C. Wang, Z.Y. Yang, X.W. Li, C.Z. Li, Synthesis of poly(aniline-co-o-anisidine)-intercalated graphite oxide composite by delamination/reassembling method, Carbon, 43 (2005) 2564–2570.
[23] A.B. Bourlinos, D. Gournis, D. Petridis, T. Szabo, A. Szeri, I. Dekany, Graphite oxide: chemical reduction to graphite and surface modification with primary aliphatic amines and amino Acids, Langmuir, 19 (2003) 6050–6055.
[24] K. Morishige, T. Hamada, Iron oxide pillared graphite, Langmuir, 21 (2005) 6277–6280.
[25] C. Petit, T.J. Bandosz, MOF–graphite oxide nanocomposites: surface characterization and evaluation as adsorbents of ammonia, J. Mater. Chem., 19 (2009) 6521–6528.
[26] P. Bradder, S.K. Ling, S.B. Wang, S.M. Liu, Dye adsorption on layered graphite oxide, J. Chem. Eng. Data, 56 (2011) 138–141.
[27] W.S. Hummers, R.E. Offeman, Preparation of graphitic oxide, J. Am. Chem. Soc., 80 (1958) 1339–1347.
[28] Z.Q. Zhu, H.X. Sun, X.J. Qin, L. Wang, C.J. Pei, L. Wang, Y.Q. Zeng, S.H. Wen, P.Q. La, A. Li, W.Q. Deng, Preparation of poly(acrylic acid)–graphite oxide superabsorbent nanocomposites, J. Mater. Chem., 22 (2012) 4811–4817.
[29] H.K. Jeong, M.H. Jin, K.P. So, S.C. Lim, Y.H. Lee, Tailoring the characteristics of graphite oxides by different oxidation times, J. Phys. D Appl. Phys., 42 (2009)1–6.
[30] X. Xue, J. Xu, S.A. Baig, X. Xu, Synthesis of graphene oxide nanosheets for the removal of Cd(II) ions from acidic aqueous solutions, J. Taiwan *Inst. Chem.* Eng., 59 (2016) 365–372.
[31] F.Y. Wang, H. Wang, J.W. Ma, Adsorption of cadmium (II) ions from aqueous solution by a new low-cost adsorbent—Bamboo charcoal, J. Hazard. Mater., 177 (2010) 300–306.
[32] D.L. Zhao, S.J. Feng, C.L. Chen, S.H. Chen, D. Xu, X.K. Wang, Adsorption of thorium(IV) on MX-80 bentonite: effect of pH ionic strength and temperature, Appl. Clay Sci., 41 (2008) 17–23.
[33] G. Zhao, L. Jiaxing, R. Xuemei, C. Changlun, W. Xiangke, Few-layered graphene oxide nanosheets as superior sorbents for heavy metal ion pollution management, Environ. Sci. Technol., 45 (2011) 10454–10462.
[34] Z. Guixia, R. Xuemei, G. Xing, T. Xiaoli, L. Jiaxing, C. Changlun, H. Yuying, W. Xiangke, Removal of Pb (II) ions from aqueous solutions on few-layered graphene oxide nanosheets, Dalton Trans., 40 (2011) 10945.
[35] X.K. Wang, X.P. Liu, Effect of pH and concentration on the diffusion of radiostrontium in compacted bentonite-a capillary experimental study, Appl. Radiat. Isot., 61 (2004) 1413–1418.
[36] S. Lagergren, About the theory of so-called adsorption of soluble substances, Kungl. Svenska Ventenskapsakad. Handl., 24 (1898) 1–39.
[37] Y.S. Ho, E. McKay, The kinetics of sorption of basic dyes from aqueous solution by sphagnum moss pea, Can. J. Chem. Eng., 76 (1998) 822–827.
[38] Y.S. Ho, G. McKay, Pseudo-second order model for sorption processes, Process Biochem., 34 (1999) 451–465.
[39] Y.S. Ho, G. McKay, Application of kinetic models to the sorption of copper (II) on to peat, Adsorp. Sci. Technol., 20 (2002) 797–815.
[40] A.O. Dada, A.P. Olalekan, A.M. Olatunya, O. DADA, Langmuir, Freundlich, Temkin and Dubinin–Radushkevich isotherms studies of equilibrium sorption of Zn^{2+} unto phosphoric acid modified rice husk, J. Appl. Chem., 3 (2012) 38–45.
[41] A. Chen, S. Chen, Biosorption of azo dyes from aqueous solution by glutaraldehyde-crosslinked chitosans, J. Hazard. Mater., 172 (2009) 1111–1121.
[42] M. Horsfall, A.I. Spiff, A.A. Abia, Studies on the influence of mercaptoacetic acid (MAA) modification of cassava (Manihot sculenta cranz) waste biomass on the adsorption of Cu^{2+} and Cd^{2+} from aqueous solution, Bull. Korean Chem. Soc., 25 (2004) 969–976.